CCFE
CULHAM CENTRE FOR FUSION ENERGY

UK Atomic Energy Authority

UKAEA-CCFE-PR(23)119

D A Ryan, R Martin, N B Ayed, L Kogan, A Kirk, the MAST Upgrade team

Initial progress of the magnetic diagnostics of the MAST-U tokamak

Initial progress of the magnetic diagnostics of the MAST-U tokamak

D A Ryan, R Martin, N B Ayed, L Kogan, A Kirk, the MAST Upgrade team

This is a preprint of a paper submitted for publication in Review of Scientific Instruments

Initial progress of the magnetic diagnostics of the MAST-U tokamak

D A Ryan[1], R Martin[1], N B Ayed[1], L Kogan[1], A Kirk[1], the MAST Upgrade team

[1] CCFE, Culham Science Centre, Abingdon, Oxfordshire, UK

Abstract.

MAST Upgrade has just begun its third physics campaign in April of 2023. The set of magnetic probes used to diagnose the magnetic field and currents on MAST Upgrade are described, and their calibration procedures outlined including calculation of uncertainties. The median uncertainty in the flux loops and pickup coils are calculated as 1.7% and 6.3%. The arrays of installed instability diagnostics are described and the detection and diagnosis of a specimen MHD mode are demonstrated. Plans for the improvement of the magnetics arrays are outlined.

1. Introduction

Robust and accurate measurements of currents, magnetic fields and fluxes, are of fundamental importance to the safe and productive operation of any toroidal plasma confinement device. The original MAST tokamak[1], operating from 2000 to 2013, featured a comprehensive set of magnetic diagnostics[2], able to accurately diagnose the plasma equilibrium state, as well as a wide variety of high frequency plasma oscillations. Following a thoroughly successful career[3], in 2013 work commenced to rebuild MAST. The machine now known as MAST Upgrade is designed to address some of the key challenges impeding the development of commercial fusion power: Most notably to further develop high performance plasma scenarios in low aspect ratio in order to reduce the minimum size and therefore cost of a commercial reactor, and to address the exhaust challenge by exploring novel plasma exhaust concepts such as the Super-X divertor. The Super-X divertor required the construction of upper and lower baffled divertor chambers, and the addition of 19 new poloidal field coils for enhanced plasma shaping. These additions necessitated a redesign of the magnetic diagnostic system, to enable the diagnosis of the the plasma state in the divertor chambers and main chamber.

During the initial commissioning phase and first campaign, the new magnetic diagnostics were incrementally brought online and commissioned, and utilised for machine protection and physics studies. The purpose of this paper is describe the state of the magnetic diagnostics at the start of the second physics campaign. In section 2 the arrays of flux loops, pickup coils and Rogowski coils used to measure the plasma equilibrium state are described. Section 3 details the in-situ calibration procedure and the resulting probe uncertainties are estimated. Section 4 describes the current status and future prospects of the MAST Upgrade instability array, and demonstrates its use for detecting and diagnosing MHD activity. Section 5 discusses the near and medium term plans for improvements to the diagnostic, to be implemented for subsequent campaigns.

2. Equilibrium Measurements

2.1. Poloidal Flux Loops

A poloidal flux loop is a single-core cable arranged as a single turn toroidal loop at a specific poloidal position, for measuring the poloidal flux at that point. A time varying flux enclosed by this loop will induce a voltage across the loop ends (known as the loop voltage), which is time integrated in hardware and then digitised. MAST-Upgrade features 102 flux loops, the locations of which are plotted in figure 1, and also available on the MAST-U visualiser[4]. The flux loops consist of a single loop of insulated wire with twisted pair tails. The wire used is either 0.3mm PEEK 1000[5] insulated copper wire or an equivalent 0.5mm diameter polythermaleze-2000 insulated copper wire, threaded through either PEEK 1000 or PTFE

Type	Cross section	Winding	NA
A	2.9x25.5mm rect.	2 layers of 71	0.0105 m2
B	2.2x27mm rect.	2 layers of 71	0.00843 m2
C	18mm diam. circ.	6 layers of 4	0.0244 m2

Table 1. Table enumerating the pickup coil types deployed in MAST Upgrade. Figures 1 and 2 show their locations.

tubing (both wire and sleave types have equivalent thermal and electrical performance). The majority of the flux loops are completely protected from the plasma by graphite armour tiles, and so the plastic tubing is sufficient. However the graphite tiles protecting the flux loops mounted on the P5 and P6 do not provide toroidally contiguous protection, so these flux loops are instead are threaded through stainless steel tubing.

Flux loops on the D1, D2, D3 and Dp coils (see figure 1 and reference [4] for coil locations) have the additional purpose measuring the vertical forces endured by these coils for machine protection. For each of these coils, 4 flux loops are installed on the rectangular coil cases, one on each corner. By subtracting the upper two signals from the lower two, the radial B field Br can be computed. This summation is performed in real time in hardware, and the signals forwarded to the real time protection system. These signals are then combined with the coil current measurements from external rogowskis to compute the JxB force on these coils. The uppermost and lowermost flux loop on the centre column serve the same purpose for the P1 coil.

As well as flux measurements, the un-integrated loop voltage measurements are also routinely used by tokamak operators. Prior to MU03, due to limited digitiser channels the loop voltage signals were produced by time differentiating and smoothing the flux measurements in software. Commencing in MU03 direct un-integrated measurements of the centre column loop voltages are now also available. By dividing a loop voltage measurement by an effective resistance, the current in toroidal structures adjacent to the flux loop can be deduced, and the vessel current thereby computed. The effective resistances were computed using VALEN 3D as previously reported[6], and the resulting vessel currents are used in the plasma current calculation (discussed in section 3.2).

2.2. Pickup Coils

Pickup coils are small multi-turn coils, used to measure one vector component of the magnetic field at a single point in (R,Z,ϕ). MAST-U pickup coils consist of a former (of which three different shapes are used, enumerated in table 1), around which is wound a 0.366mm diameter PEEK 1000 insulated copper wire.

These coils are held in mounts of PEEK 1000 (a plastic material with a maximum continuous service temperature of 250C, sufficient to withstand vessel bake conditions),

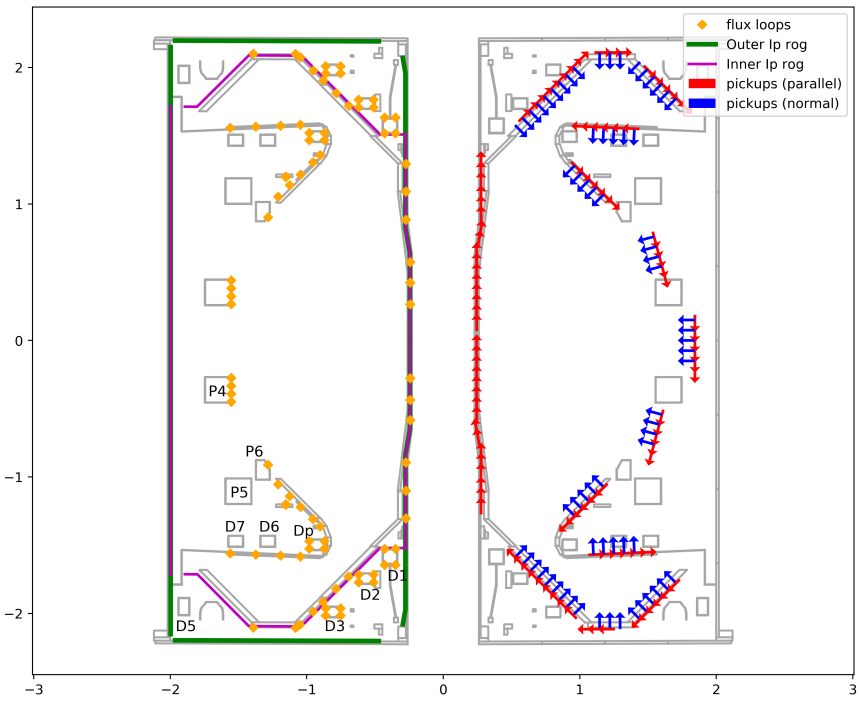

Figure 1. Sketch of the poloidal arrays of pickup coils and flux loops, as well as paths of the two types of plasma current rogowski. Note that the toroidally opposite pairs of each plasma current rogowski, and toroidally opposite pairs of each pickup coil, are not shown for clarity. The UKAEA hosts an interactive browser where the MAST-U geometry may be visualised [4].

and arranged into cassettes of several coils in alternating orientations as shown in figure 2, enclosed in a covering of 0.5mm stainless steel. Unlike the other cassettes, the outboard midplane cassettes are not beneath any graphite vessel armour tiles, so require their own 6mm graphite armour covers. Using the formula below (yielded by inverting the well known skin depth formula [7]) a wall frequency f_w can be computed, above which signals are attenuated by an electrically conducting covering.

$$f_w = \rho/(\pi\mu_0\mu_r w^2) \tag{1}$$

where ρ, w, μ_r are the electrical resistivity, covering thickness, and relative permeability of the material. The 316L steel used in the 0.5mm cassette covers has ρ=0.74 $\mu\Omega m$ and μ_r=1.008, which yields f_w=0.74MHz. The graphite armour has a higher resistivity (notoriously varying, but approximated here as 50 $\mu\Omega m$), but nonetheless has a comparable wall frequency of 0.35 MHz due to larger thickness. Therefore in addition to diagnosing the equilibrium state, these pickup coils are able to capture MHD modes of frequencies exceeding

100kHz, as discussed in section 4 of this report. Such cassettes are arranged in arrays proving near complete poloidal coverage with 354 pickups in total measuring the poloidal field, as shown in figures 1 and 2 (in practice a smaller number are typically operating, discussed in section 3). The locations and orientations of these coils are available via the MAST-U geometry visualizer[4].

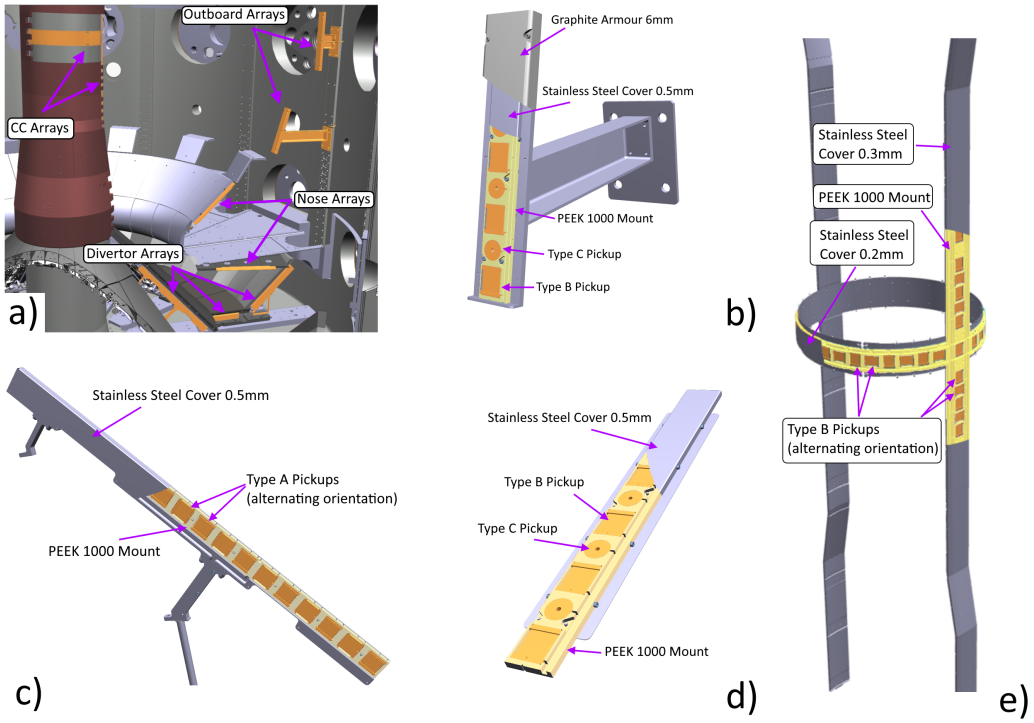

Figure 2. a) Sketch of the lower interior of MAST Upgrade, with the pickup coil arrays highlighted. b) Sketch of an outboard pickup cassette, which is covered by a stainless steel cover and 6mm graphite armour. c) Sketch of a divertor pickup cassette. d) Sketch of a cassette mounted on the divertor baffle and nose. e) The array of pickups mounted on the center column.

2.3. Coil Rogowskis

Rogowski coils are multi-turn coils conceptually similar to pickup coils, except the coil is curved into a loop, used to measure the current the loop encloses. The current supplied to each poloidal field coil of MAST Upgrade is measured by a Rogowski around each coil feed. On MAST-Upgrade all toroidally flowing currents (including any coil currents or plasma currents) flowing anti-clockwise viewed from above are defined as positive. All PF coils except P1, Px and Pc are in-vessel coils, and so require cases to separate them from vacuum. These coil cases are toroidally contiguous, and so can support substantial induced toroidal currents. Therefore each of these coil cases is enclosed by 4 separate in-vessel Rogowski coils which measure the sum of coil and case current. These internal coil rogowskis secured directly to the coil cases, the poloidal coordinates of which are available via the MAST-U geometry visualizer[4]. By

subtracting the feed current measured by the external rogowskis (multiplied by the number of coil turns) from the total current measured by the internal rogowskis, the coil case currents are computed.

2.4. Plasma Current Rogowskis

MAST-U features 2 types of plasma current rogwoskis: outer rogowskis whose path traces the outermost extents of the vacuum vessel (mounted on the vacuum side), and inner rogowskis whose path takes a short cut under the divertor tiles, thereby excluding several divertor PF coils. The outer sets of rogowskis enclose all in-vessel coils, while the inner sets of rogowskis exclude PF coils D1, D2, D3, and D5. Figure 1 shows the poloidal paths of each rogowski. In the figure the rogowskis are sketched at only one value of toroidal angle but in fact they both have an identical set on the opposite side of the machine, 180 toroidal degrees apart (not shown for clarity, since it would obscure the pickup coils). Each of these 4 rogowskis is split into 4 separate segments (inboard vertical, outboard vertical, upper horizontal and lower horizontal), producing 16 separate signals in total. The total current enclosed by the rogowskis is computed as a weighted sum of the individual segments, whose weights are computed by a calibration procedure described in section 3.2. The sum of the enclosed coil currents, computed vessel current, and TF pickup are all subtracted from this sum of rogowski segments, to yield the plasma current.

2.5. Integrators and digitisers

All sensors here described function by the measurement the voltage induced by a time varying magnetic field, and therefore require time integration to yield the magnetic flux. Since in MAST-U these signals are needed in real-time for use by the plasma control and real-time protection systems, this time integration is performed in hardware. The MAST Upgrade plasma control system is previously reported elsewhere[8]. Two integrator designs are in use on MAST Upgrade, both of which have a $10k\Omega$ input impedance, chosen to be substantially larger than the probe impedances which are typically less than 10Ω. The first type outputs a time integrated analogue signal which can then be streamed in real-time to the plasma control and real-time protection systems, and is separately digitised by a 16 bit digitiser. The second type has an integrated 16 bit digitiser, but cannot forward real-time data to downstream users (although this functionality is envisaged for future campaigns to increase the number of signals available to the plasma control system). Digitisation in both cases has a ± 10 V voltage range, which yields a digitisation precision of 0.3mV. For typical calibration factors this translates to a precision of around 0.3mT for pickup coils and 0.1mWb for flux loops, which is far lower than the uncertainty in these probes as calculated in section 3.

3. Calibration

The time integrated measurements of flux loops, pickup coils and Rogowski coils described above, all require calibration factors to convert the voltage measurements into Webers (for flux loops), Tesla (for pickups) or Amperes (for the Rogowskis). In MAST Upgrade, all internal magnetics are calibrated in-situ using the external rogowskis as references, which are themselves calibrated by the manufacturer to an uncertainty of 0.1%. Since all internal probes are calibrated relative to these external rogowskis, this value of 0.1% represents the floor of the achievable uncertainty for any internal magnetic diagnostic. In practice the achieved uncertainty is substantially higher than this, as explained below.

3.1. Flux loops and pickup coils

The in-situ calibration procedure for flux loops and pickup coils is as follows. In a dedicated set of vacuum shots, each poloidal field coil is fired separately with a trapezoidal current waveform, which has a sufficiently long flattop to allow all eddy currents to attenuate to negligible levels. Experience has shown 200 ms is sufficient for this, but the flattops are typically on the order of 1s long. Since induced eddy currents are excluded, predictions of the sensor readings during the stationary flattop can be made with a DC vacuum model. Each probe i has calibration factor α_i, calculated independently of each other. For each of the vacuum shots j, a measurement of the set of $\alpha_{i,j}$ is taken as $\alpha_{i,j} = P_{i,j}/O_{i,j}$, where $P_{i,j}$ and $O_{i,j}$ is the predicted reading (in physics units, T or Wb) and observed reading (in Volts) for probe i and calibration shot j. The calibration factor for a given probe α_i is then taken as the arithmetic median over calibration shots j. The uncertainty for each α_i is taken as the standard deviation over j. Note that the median over j is used rather than the mean, since this measure is more robust to instances where a sensor is particularly close a specific coil, which can cause small defects in the as-installed position and orientation to be magnified for the vacuum shot in which this coil is fired. To mitigate the effects of high uncertainty probes on downstream calculations (in particular, EFIT reconstructions), probes with calibration uncertainties above a (somewhat arbitrarily chosen) limit are excluded by the inter-shot analysis code. The limits applied in MU01 and MU02 were $0.02Wb/V$ for flux loops and $0.2T/V$ for pickup coils. The filtered calibration factors and uncertainties are plotted in figure 3. After applying this filter, 234 pickup coils (out of 354 total) and 95 flux loops (out of 102 total) remain for analysis. The median uncertainty of the remaining flux loops and pickup coils is 1.7% and 6.3% respectively. Since flux loops provide a toroidally averaged measurement of a scalar field, they are less sensitive to local irregularities and therefore tend to be more accurate than point measurements of a vector field provided by pickup coils, which is reflected in the higher uncertainties of the MAST Upgrade pickup coils. The inter-shot analysis code applies the computed calibration factors to each signal, removes integrator drift and offset, removes TF pickup, and writes the resulting calibrated signals to the MAST-U data archive. It is envisaged that methods for computing probe calibrations and their uncertainties will continue to be

refined as the MAST Upgrade programme continues, in particular following the processes outlined in [9, 10].

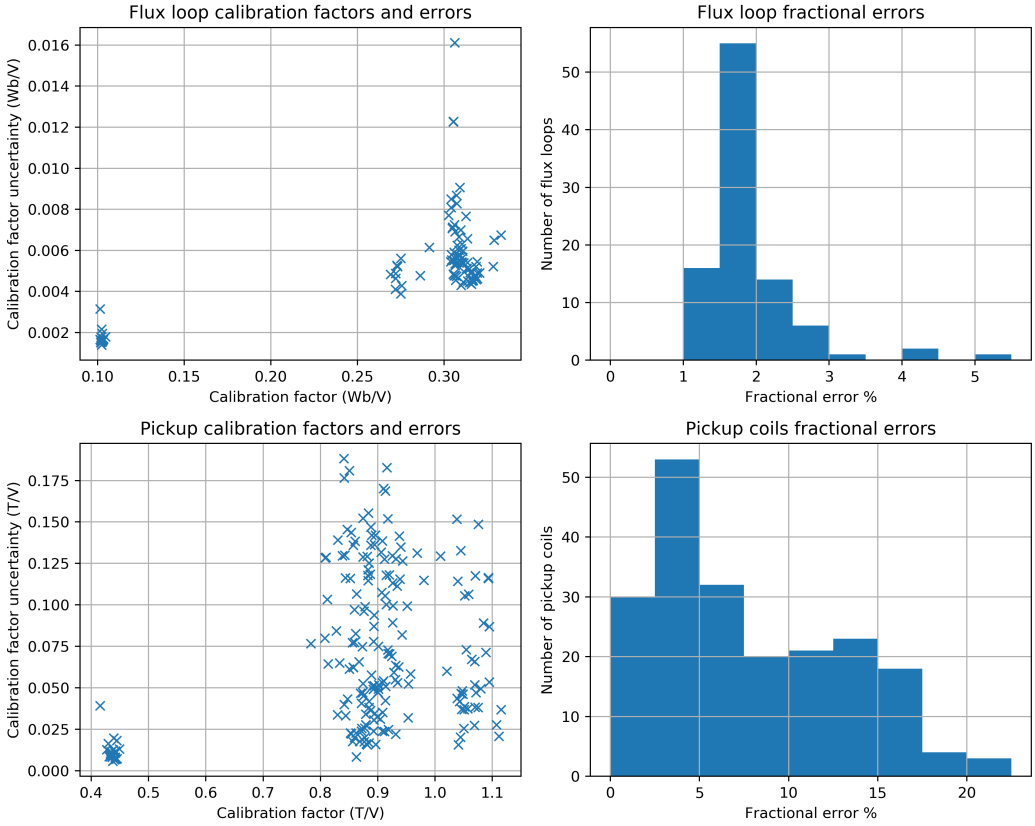

Figure 3. a) Calibration factors of the flux loops against their uncertainties. There are two groups on this plot because two types of voltage dividers are applied to the flux loops, which are required to keep the measurements within the integrator voltage rails. b) A histogram showing the fractional error of the flux loop calibration factor, which indicates the fractional error on the flux loops. The median is 1.7%. c) Calibration factors of the pickup coils against their uncertainties. These are also in two groups, because the centre column pickups are summed with their toroidally opposite counterpart prior to integration. d) A histogram showing the fractional error of the pickup coil calibration factor, which indicates the fractional error on the flux pickup coils. The median is 6.3%. Any probe with a measured uncertainty exceeding 0.2T/V is excluded from further analysis, and so not included in the above.

3.2. Plasma Current Rogowskis

This same set of vacuum shots is also used to calibrate the plasma current rogowskis. Because the plasma current rogowskis do not form a contiguous loop around the poloidal cross section but are instead each comprised of 4 segments (each producing signal x_k), the measurement of the enclosed current Ip is calculated as a weighted sum of these segments:

$$Ip = \alpha_{Ip} \Sigma_k [\beta_k x_k] \tag{2}$$

where β_k are the segment weights, normalised such that $\Sigma_k \beta_k = 1$. First the weights β_k are computed by comparing the measured signals from each segment to modelled segments for each vacuum shot. In the same way as the pickups and flux loops are calibrated, each vacuum shot produces an independent measurement of β_k, and the final values are then taken as the median over the vacuum shots. Next the factor α_{Ip} is computed as

$$\alpha_{Ip} = \Sigma[I_c] / \Sigma_k[\beta_k x_k] \tag{3}$$

where $\Sigma[I_c]$ is the sum of the currents of the enclosed poloidal field coils measured by the external rogowskis. The value and uncertainty of α_{Ip} are taken as the median and standard deviation over the vacuum calibration shots. This measure yields an uncertainty in the Ip calibration factors of approximately 3%.

Slight installation defects in all these sensors cause them to also detect a small component of the toroidal field. This TF pickup is measured using a TF vacuum shot, and subtracted prior to application of the calibration factors. In the case of all the diagnostics described here, intershot analysis codes process the raw signals by subtracting TF pickup and integrator drift, and applying the computed calibration factors before saving the processed signals for further physics analysis. For example, during MU01 the above set of magnetics diagnostics was used routinely to produce magnetically constrained equilibrium reconstructions using the EFIT++ code, and good agreement with independent diagnostic measurements was demonstrated [11].

4. Instability magnetics

For detecting and diagnosing MHD instabilities, a comprehensive set of instability diagnostics is installed in MAST Upgrade. This consists of three rows of outboard saddle coils and two rows of centre column saddle coils, all providing full toroidal coverage. The pickup coils described in section 2.2 may be both collected via an integrator and also digitised separately before integration, allowing these probes to function both as low frequency magnetic field measurements (referred to as pickups) and also high frequency instability sensors (usually referred to as Mirnov coils). Similarly the saddle coils are digitised as both integrated signals for diagnosing slowly growing instabilities such as locked modes, and un-integrated signals for diagnosing rapidly rotating global MHD modes. These instability diagnostics are digitised at 200kHz, which is quite sufficient given that frequencies above this are expected to be attenuated by local vessel armour as described in 2.2. The full set of installed instability diagnostics are plotted in figure 4. Using the outboard saddle coil toroidal arrays, toroidal mode numbers of detected modes can readily be determined. Figure 5 demonstrates a global MHD mode detected at 11.8kHz during beam heated discharge 46445 during MU02. This mode is plainly visible on all the diagnostics plotted in 4, and therefore the toroidal mode number can be trivially determined by measuring the rate of change of the phase of the mode

with toroidal angle. Due to limited digitiser channels not all the instability diagnostics plotted in figure 4 could be fully commissioned prior to MU02, which made poloidal mode number determination impractical. The installation of an additional digitiser after MU02 has allowed more of the installed Mirnov coils to be added to the poloidal array, greatly extending its poloidal coverage. Therefore the measurement of poloidal mode numbers of detected modes is anticipated to be routine in MU03, which is scheduled to commence in April 2023.

4.1. OMAHA coils

The OMAHA diagnostic is an array of Mirnov coils whose frequency characteristics are optimised for the detection of high frequency toroidal modes[12]. In contrast to the other Mirnovs which sit behind thick graphite tiles, the OMAHA coils are protected by a 3mm aluminium oxide ceramic sheath coated with a thin layer of colloidal graphite paint. The very high wall frequencies of these protective layers allow these coils to detect frequencies well into the MHz range. Other than slight alterations to their locations they are unchanged from their deployment on MAST, which is described in detail previously[12]. Figure 6 demonstrates a typical target mode for the OMAHA coils, in this case an Alfven Eigenmode at around 2MHz. Toroidal mode number determination is also possible using the OMAHA array, but this is not performed here.

5. Discussion and Outlook

This paper describes the current state of the Mast Upgrade magnetic diagnostics just prior to the third campaign. While very far from matured, they have provided vital machine and plasma informations to facilitate the first campaigns, notably facilitating equilibrium reconstructions which agree well with independent diagnostics, as well as reliably providing essential signals for plasma control, and for basic machine operation and protection. Nonetheless, the progress reported here represents only the start of the development of the MAST Upgrade magnetic diagnostics, all aspects of which having significant scope for improvement. Most notably, the calibration procedures used in the initial MAST Upgrade campaigns are in general over simplistic and should be brought in line with modern rigorous standards, following [10].

During MU02, there were insufficient digitiser channels to collect all the instability diagnostics, making determination of poloidal mode numbers of detected MHD modes impractical. During the engineering break prior to MU03, the poloidal coverage of the Mirnov coil array has been extended (specified in figure 4) to facilitate diagnosis of the poloidal mode numbers of detected MHD modes. This facility is expected to be employed routinely in MU03, commencing in April 2023. Currently the saddle coils are all integrated and digitised individually, so the measured signal is dominated by the n=0 equilibrium component, making

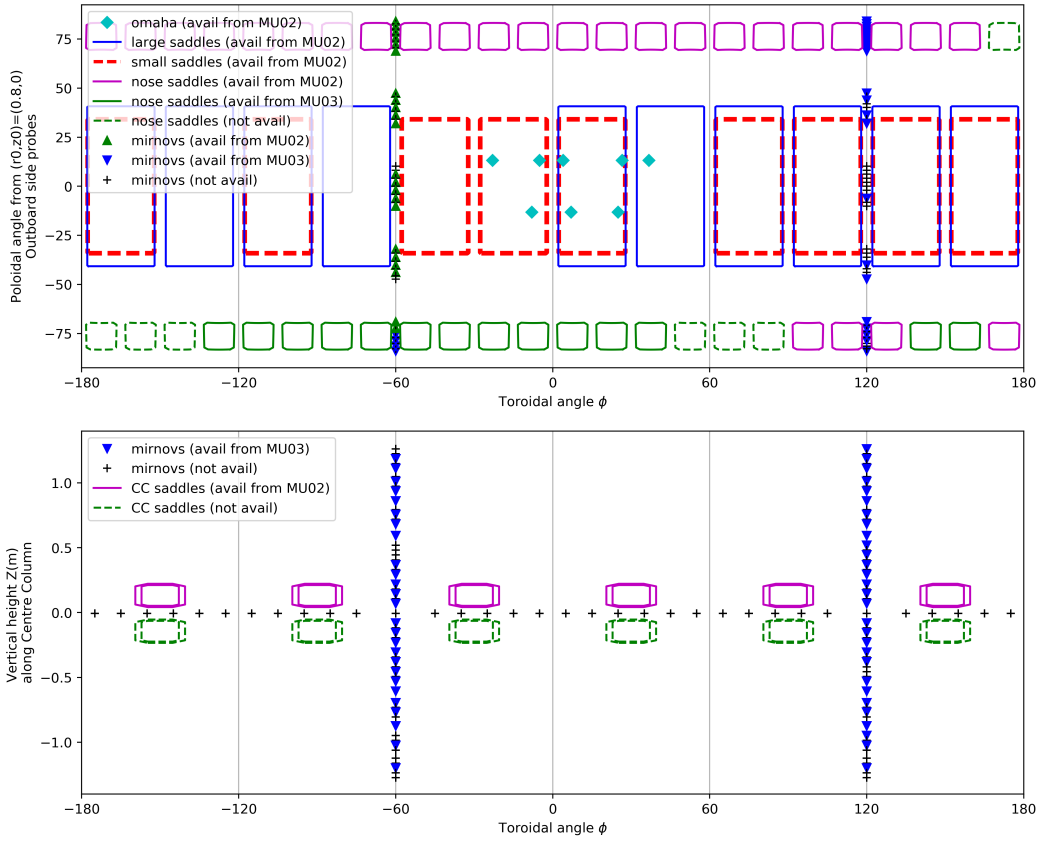

Figure 4. a) Sketch of the as-designed 3D sensor locations on the outboard side. Due to insufficient digitisation channels not all the probes can be collected. b) Sketch of the as-designed 3D sensor locations on the centre column. The CC vertical Mirnovs are digitised starting in MU03.

it difficult to extract higher n slowly varying 3D fields such as those of interest to RMP plasma response studies[13]. It is envisaged that in the future the outboard saddle loop array will be reconfigured as a set of differenced pairs following [14], such that slowly varying fields may be accurately diagnosed.

The median uncertainty in the flux loops is 1.7%, which is considered adequate. However the accuracy may be improved further following [10], by subtracting a reference flux loop in hardware to eliminate the contribution of the central solenoid, to improve the dynamic range of the flux loop array.

Of the 354 poloidal field pickup coils installed in MAST Upgrade, only 234 (65%) are routinely used in the first campaigns, mostly due to the uncertainty on their calibration factor exceeding the limit 0.2T/V, which was applied to limit the uncertainty in data entering the analysis stream. Of these that remain, the median calibration uncertainty is 6.3%, but can range up to 15-20%, which is considered wildly excessive and should be urgently addressed in future works. To generate the predicted readings used in the calibration procedure, accurate and precise knowledge of the location and orientations of each probe relative to the PF coils

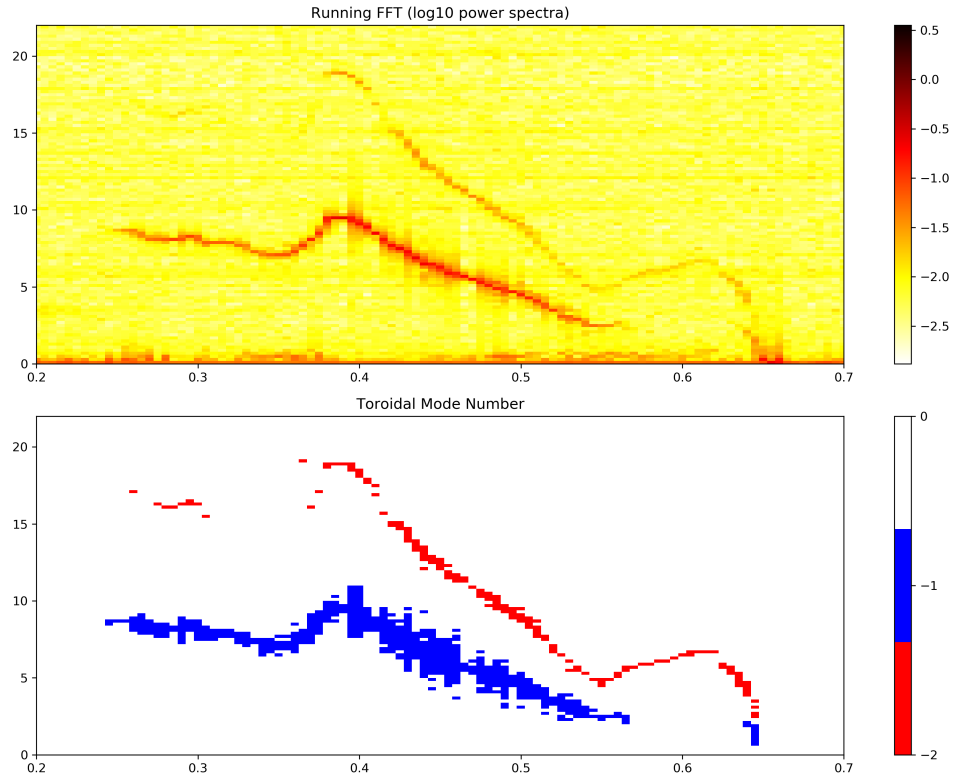

Figure 5. a) Frequency spectrogram showing an example global MHD mode in a typical beam heated MAST-U discharge. The physics of this mode are not discussed in this paper, which merely aims to demonstrate their detection and diagnosis. b) This figure plots the phase of this mode as measured by the outboard saddle coils, against the toroidal angle of the saddle coils, revealing the toroidal mode number of the mode. Global MHD up to 100kHz is visible on all the commissioned probes and saddle coils sketched in figure 4. Having complete toroidal coverage allows ready determination of MHD toroidal mode numbers, as demonstrated here.

is required, and therefore small deviations between the as-designed and as-built sensors and PF coils can result in substantial errors in the probe calibrations. It is envisaged that these errors may be reduced by an optimisation procedure which minimises the calibration error by slightly varying the simulated probe locations and orientations to better reflect their likely as-built counterparts, as in [9]. This procedure would increase the utility of the MAST Upgrade pickup coil arrays by reducing the calibration uncertainties, and perhaps also yield information on the deviations from axi-symmetry in the poloidal field, which would assist error field studies.

The in-situ calibration procedure ultimately derives calibration factors from the external rogowski calibration factors, so all magnetics calibrations share a dependency on the external rogowski coils calibration. Having a separate and independent measure of the magnetic field would therefore be of great value to the MAST Upgrade magnetics system, to eliminate this single dependency, and options for providing this are being explored.

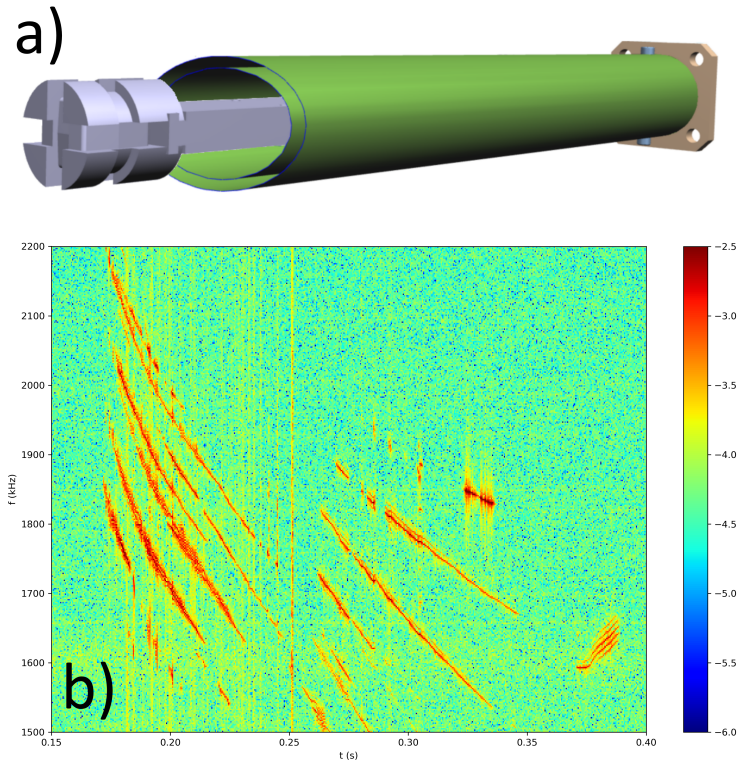

Figure 6. a) Sketch of an OMAHA probe. The bobin on the end supports 3 coils, wound to measure 3 orientations separately. The ceramic cover and thin graphite paint armour has a negligable shielding effect allowing frequencies in the MHz range to be measured. b) An example of a target mode at 2MHz, from a typical beam heated MAST-U discharge.)

Acknowledgements

This work has been funded by RCUK Energy Programme (grant number EP/P012450/1). To obtain further information on the data and models underlying this paper please contact PublicationsManager@ukaea.uk.

References

[1] M. Cox, 1999, *Fusion Engineering and Design*, **46**, 397–404.
[2] T. Edlington *et al*, 2001, *Review of Scientific Instruments*, **72**, 421–425.
[3] J.R. Harrison *et al*, 2019, *Nuclear Fusion*, **59**, 112011.
[4] UKAEA. *MAST-U Geometry Visualiser*, 2023. `https://users.mastu.ukaea.uk/internal/mastu-visualiser` (Accessed 06.03.2023).
[5] The Quadrant Group. *Ketron 1000 PEEK Technical Data sheet*, 2011. `www.theplasticshop.co.uk/plastic_technical_data_sheets/peek_1000_technical_data_sheet.pdf` (Accessed 03.02.2023).
[6] J. W. Berkery *et al*, 2021, *Plasma Physics and Controlled Fusion*, **63**, 055014.
[7] J D Huba. *NRL PLASMA FORMULARY Supported by The Office of Naval Research*. Naval Research Laboratory, Washington, DC, 2013.
[8] Graham McArdle *et al*, 2020, *Fusion Engineering and Design*, **159**, 111764.
[9] J. M. Moret *et al*, 1998, *Review of Scientific Instruments*, **69**, 2333–2348.
[10] E. J. Strait, 2006, *Review of Scientific Instruments*, **77**, 023502.

[11] L Kogan *et al*. First MAST-U Equilibrium Reconstructions using the EFIT ++ code. In *Proc. 48th EPS Conference on Plasma Physics*, 2–5, Maastricht, 2022.
[12] M. J. Hole *et al*, 2009, *Review of Scientific Instruments*, **80**, 123507.
[13] S. Munaretto *et al*, 2018, *Physics of Plasmas*, **25**, 072509.
[14] S. Munaretto *et al*, 2021, *Review of Scientific Instruments*, **92**, 073504.